Transition Metal Chemistry **25**: 260–264, 2000.

Catalytic activity of a zirconium(IV) oxide surface supported with transition metal ions

Ibrahim A. Salem*, Rania I. Elhag and Kamal M. S. Khalil
Chemistry Department, Faculty of Science, UAE University, Al-Ain, P.O. Box 17551, UAE

Received 29 June 1999; accepted 14 July 1999

Abstract

The kinetics of H_2O_2 decomposition have been investigated using ZrO_2 supported with transition metal ions including Cu^{II}, Ag^{I}, Hg^{II}, Co^{II}, Mn^{II}, Ni^{II} and Fe^{III}. At pH = 6.8, the reaction rate exhibits a first order dependence on the initial H_2O_2 concentration at low concentrations. The order of activity of the different catalysts is strongly dependent on the $[H_2O_2]_0$ used. The reaction proceed *via* the formation of the peroxo-intermediate which has an inhibiting effect on the reaction rate. The rate increases with increasing pH, and attains a limiting rate at higher pH's. A reaction mechanism is proposed involving liberation of $HO_2^{\bullet}$ radicals from the peroxo-intermediate as the rate-determining step.

Introduction

The use of hydrogen peroxide, a powerful oxidant, has increased dramatically in the past few years. The only byproducts formed are water and oxygen, thus it is often referred to as a friendly oxidant. Hydrogen peroxide can be used directly (uncatalyzed) [1–3], for simple oxidations, or in conjunction with an activator (catalyzed), u.v. light or ozone for advanced and complex oxidation processes [4–38]. These reactions have been carried out in both homogeneous [4–10, 37, 38] and heterogeneous [11–30] media.

Many contributions have been made to the heterogeneous catalytic decomposition of hydrogen peroxide on the surface of metal oxides [11–19], iron containing minerals [15] and polymers supported by metal ions or their complexes [20–30]. On the other hand, silica–alumina, and silica gel supported with copper(II), cobalt(II), manganese(II) and iron(III) as well as some of their complexes, were used in the decomposition of hydrogen peroxide [16–19]. The reaction rate decreases in the order: copper(II) > cobalt(II) > iron(III) [16], however, the rate increases with the basicity of the ligand [18, 19].

Polymers and ion-exchange resins immobilized with transition metals and complexes were used to decompose hydrogen peroxide catalytically [20–30]. The kinetics of the decomposition with cobalt(II) and copper(II) porphyrins complexes were studied and the reaction was found to be first order in both substrate and catalyst [20]. Ammonia, amines and bis-salicylaldimine Schiff-base ligands are strongly sorbed by the Dowex-50W resin supported with different metal ions [24–30]. The activity of these catalysts was found to be strongly dependent on the metal, the ligand and both DVB% and mesh size of the resin. On the other hand, ZrO_2 supported copper, iron or both showed high activity and selectivity for the reaction between NO and CO [31, 32]. Recently, ZrO_2/Cu^{2+} was reported to be effective for NO reduction by hydrocarbons in the presence of oxygen [32]. It also exhibits high activity and selectivity for MeOH formation from CO_2 and H_2 [34–36]. Degassing zirconium oxide at high temperatures led to abnormal absorption and photoluminescene associated with the presence of low coordinated surface sites used for CO adsorption [37]. The present work pertains to the study of the heterogeneous decomposition of hydrogen peroxide on the surface of zirconium(IV) oxide supported with transition metal ions. We are now using this system to remove the colour from organic dyes, which is very useful in waste water treatment.

Experimental

Materials and reagents

All chemicals used were of analytical reagent grade quality. H_2O_2 solutions were prepared by direct dilution and standardized iodometrically using sodium thiosulphate.

Zirconia-immobilized with transition metal ions

ZrO_2 (Merck; granules patinal, particle size *ca.* 0.5–2 mm) was washed repeatedly with redistilled H_2O, dried and activated at 150 °C for 24 h. The required amount of activated zirconia was kept in contact with the solution of metal sulphate (10^{-3} M) for 24 h.

* Author for correspondence

Zirconia in the metal ion form was then filtered and washed repeatedly with redistilled H_2O until free from any excess of metal sulphate solution.

Physical measurements

An atomic absorption spectrometer 906 GBC AA in conjunction with a graphite furnace (GF 3000) and hydride generator (HG 3000) was used to determine the amount of metal ions adsorbed per gram of the catalyst. This was done after bleaching the supported metal ions with HNO_3. The amount (mg) of metal ion per g of catalyst for Ag^{I}, Cu^{II}, Hg^{II}, Co^{II}, Mn^{II}, Fe^{III} and Ni^{II} is 0.53, 3.56, 0.32, 0.91, 2.51, 0.76 and 1.96 respectively. A philips X-ray diffractometer model PW/1840, with Ni filter, Cu$K\alpha$ radiation (λ = 1.542 Å) at 40 kV, 30 mA and scanning speed 0.02° s^{-1} was used for XRD measurements. A SEM Jeol JSM-5600 was used for recording micrographs. pH measurements were made employing Mettler Delta 320 pH-meter, and phosphate buffer was used throughout.

Kinetic measurements

Kinetic measurements were carried out following the procedure previously described [24, 25]. The measurements were confined to 30 °C. The observed rate constant, k_{obs}, was evaluated from the integrated first order equation.

Results and discussion

Characterization of the different catalysts

The unsupported and supported zirconia samples were examined by X-ray powder diffraction in order to identify the crystallinity of the unsupported material and to detect any crystalline phases developed. Figure 1 shows the XRD pattern of the unsupported zirconia together with the copper(II) and iron(III) supported samples as representative for the supported samples. Indexing of the patterns [38] indicated that the unsupported zirconia crystallizes as a baddeleyite phase of ZrO_2. Typical diffraction patterns were observed for all the supported samples, indicating that baddeleyite was the only crystalline phase present. Thus supporting zirconia, according the procedure described above, has induced no appreciable phase modification. On the other hand, zirconia granules were examined before and after loading. Figure 2A illustrates the case of unsupported zirconia granules. Photographs recorded for the supported samples showed micrographs similar to that of pure zirconia, Figure 2B. This confirms that, no effects other than sorption have occurred.

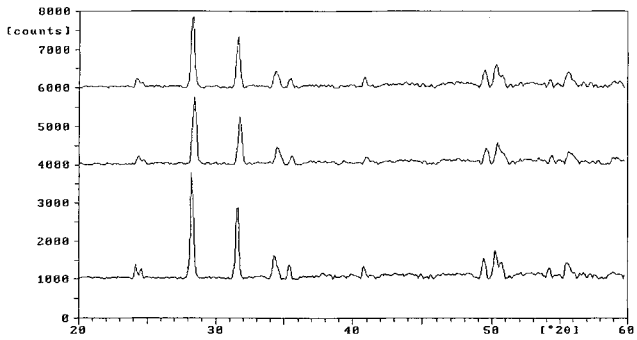

Fig. 1. XRD diffractogram of the unsupported zirconia (lower) Cu^{II} supported (middle) and Fe^{III} supported (upper).

Reaction with hydrogen peroxide

Experiments carried out using activated zirconia before support with transition metal ions showed a very slow reaction with hydrogen peroxide even at high pH's. For this reason, we used transition metal ion sulphate for a comparative study. Experiments were carried out at pH = 6.85 and 30 °C with 1 g of air-dry catalyst (Figure 3). By inspection of Figure 3, we can easily see that, the rate of decomposition increases gradually with increasing $[H_2O_2]_0$ reaching a maximum, then decreasing. This behaviour was ascribed to the formation of an intermediate active species, which has an inhibitory effect on

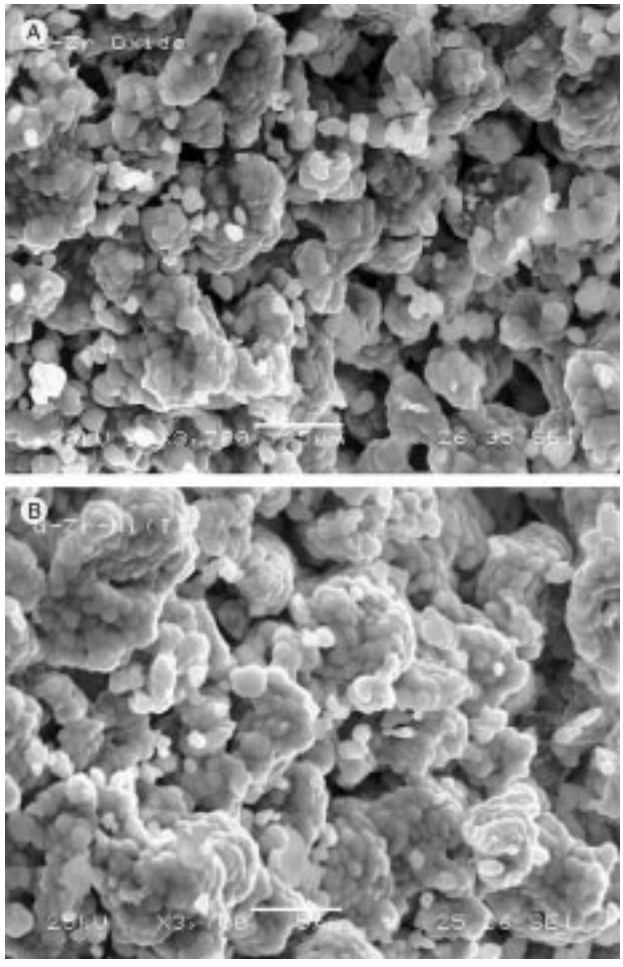

Fig. 2. (A) SEM micrograph for the unsupported zirconia catalyst. (B) SEM micrograph for the nickel(II) supported zirconia catalyst.

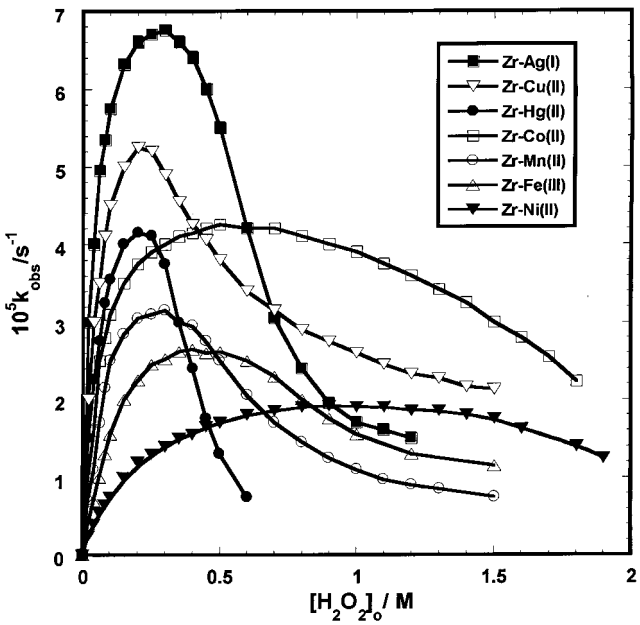

Fig. 3. Variation of the observed rate constant with the initial concentration of H_2O_2 for its decomposition with 1 g of zirconia catalysts at pH = 6.85 and 30 °C.

the reaction rate [16]. With most of these catalysts, this intermediate has a specific colour. The formation of a brown intermediate, which is significant for copper, was found at $[H_2O_2]_0 > 0.2$ M. At higher $[H_2O_2]_0$, the formation of such an intermediate becomes more significant and the reaction rate remarkably decreased. From the same Figure, it is also clear that the rate of reaction has a first order dependence on $[H_2O_2]_0$, only before the formation of such intermediate began. As $[H_2O_2]_0$ increases, the formation of the intermediate commenced and the reaction order decreases until it reached zero at the maximum rate, then became negative at higher $[H_2O_2]_0$.

The reactivity order for the different catalysts is strongly dependent on the hydrogen peroxide concentration. At lower $[H_2O_2]_0$, before the formation of the inhibitory intermediate, the order is: $Ag^{I} > Cu^{II} > Hg^{II} > Co^{II} > Mn^{II} > Ni^{II} > Fe^{III}$. This order is better correlated with both the amount of the metal ion loaded and its redox potential. Comparing Ag^{I} with both Mn^{II} and Ni^{II} reveals that, the redox potential has the pronounced effect. However, at higher $[H_2O_2]_0$, the order of reactivity is different, see Figure 3. This may be ascribed to the difference in the amount of hydrogen peroxide required for the formation of the intermediate active species; *e.g.* cobalt (II) needs more hydrogen peroxide than copper(II), (Figure 3).

According to the above discussion, we postulate the decomposition mechanism as follows;

$$H_2O_2 \overset{K_1}{\rightleftharpoons} HO_2^- + H^+ \tag{1}$$

$$Zr\text{–}M^{n+} + HO_2^- \overset{K_2}{\rightleftharpoons} \underset{\text{Peroxo-intermediate}}{Zr\text{–}M^{n+}(HO_2)^-} \tag{2}$$

After the formation of the peroxo-intermediate, the reaction may propagate *via* a one electron oxidation step with the liberation of an $HO_2^{\bullet}$ radical [9, 31], thus;

$$Zr\text{–}Mn^{n+}(HO_2)^- \xrightarrow{k_1,\text{slow}} Zr\text{–}M^{(n-1)+} + HO_2^{\bullet} \tag{3}$$

$$HO_2^{\bullet} + H_2O_2 \longrightarrow OH^{\bullet} + O_2 + H_2O \tag{4}$$

$$Zr\text{–}M^{(n-1)+} + OH^{\bullet} \longrightarrow Zr\text{–}M^{n+} + OH^- \tag{5}$$

The rate determining step in this mechanism is the conversion of M^{n+} into $M^{(n-1)+}$, (Equation 3). From Equations (1) and (2), the concentration of the peroxo-intermediate is given by;

$$[Zr\text{–}M^{n+}(HO_2)^-] = K_1K_2[Zr\text{–}M^{n+}][H_2O_2]/[H^+] \tag{6}$$

Expressing for the total initial concentration of hydrogen peroxide and the catalyst, $[H_2O_2]_0$ and $[Zr\text{–}M^{n+}]_0$ respectively, where;

$$[H_2O_2] = [H_2O_2]_0 - [Zr\text{–}M^{n+}(HO_2)^-] \tag{7}$$

$$[Zr\text{–}M^{n+}] = [Zr\text{–}M^{n+}]_0 - [Zr\text{–}M^{n+}(HO_2)^-] \tag{8}$$

therefore;

$$[Zr\text{–}M^{n+}(HO_2)^-] = \frac{K_1K_2[Zr\text{–}M^{n+}]_0[H_2O_2]_0}{K_1K_2([H_2O_2]_0 + [Zr\text{–}M^{n+}]_0) + [H^+]} \tag{9}$$

From Equation (3),

$$\text{Rate} = k_1[Zr\text{–}M^{n+}(HO_2)^-]$$

$$\text{Rate} = \frac{k_1K_1K_2[Zr\text{–}M^{n+}]_0[H_2O_2]_0}{K_1K_2([H_2O_2]_0 + [Zr\text{–}M^{n+}]_0) + [H^+]} \tag{10}$$

This equation predicts that, at constant catalyst concentration, the reaction rate increases with increasing $[H_2O_2]_0$, attaining a limiting rate at relatively high $[H_2O_2]_0$ (Figure 3). However, it cannot account for the decrease in rate at higher $[H_2O_2]_0$. This may be explained by proposing that the reaction proceed *via* the formation of a second intermediate as follows;

$$Zr\text{–}M^{n+}(HO_2)^- + H_2O_2 \overset{K_3}{\rightleftharpoons} Zr\text{–}M^{n+}(HO_2)^-(H_2O_2) \tag{11}$$

$$Zr\text{–}M^{n+}(HO_2)^-(H_2O_2) \xrightarrow{k_3} Zr\text{–}M^{(n-1)} + \frac{1}{2}O_2 + H_2O + HO_2^{\bullet} \tag{12}$$

From Equations (6–9) and (13), the concentration of the second intermediate is given by;

$$\mathrm{Zr{-}M^{n+}(HO_2)^-(H_2O_2)} = \frac{K_1^2K_2^2K_3[\mathrm{Zr{-}M^{n+}}]_0[\mathrm{H_2O_2}]_0^3 + K_1K_2K_3[\mathrm{H^+}]}{K_1K_2[\mathrm{H^+}]([\mathrm{H_2O_2}]_0 + [\mathrm{Zr{-}M^{n+}}]_0)} - \frac{K_1^2K_2^2K_3[\mathrm{Zr{-}M^{n+}}]_0^2[\mathrm{H_2O_2}]_0^2}{K_1K_2[\mathrm{H^+}]([\mathrm{H_2O_2}]_0 + [\mathrm{Zr{-}M^{n+}}]_0)} \quad (13)$$

The first and the last terms in the numerator can be omitted;

$$[\mathrm{Zr{-}M^{n+}(HO_2)^-(H_2O_2)}] = \frac{K_3}{([\mathrm{H_2O_2}]_0 + [\mathrm{Zr{-}M^{n+}}]_0)} \quad (14)$$

The rate equation becomes;

$$\mathrm{Rate} = k_3[\mathrm{Zr{-}M^{n+}(HO_2)^-(H_2O_2)}] = \frac{k_3K_3}{([\mathrm{H_2O_2}]_0 + [\mathrm{Zr{-}M^{n+}}]_0)} \quad (15)$$

Now, it is clear that at constant catalyst concentration, the reaction rate decreases with increasing $[H_2O_2]_0$ (last portion of the curve in Figure 3).

The involvement of radicals in the reaction mechanism was detected using *t*-BuOH as a radical scavenger [39, 40]. The rate of reaction was remarkably inhibited in 20% *t*-BuOH (Figure 4). The effect of pH on the reaction rate was studied at constant concentration of both the catalyst and the substrate at 30 °C. The pH varied from 4.3–10 using phosphate buffer. A few drops of sodium hydroxide were added to attain higher pH values (Figure 5). Generally, the reaction rate increased with increasing basicity, due to enhanced formation of the peroxo-intermediate in alkaline solution [31]. Equation (10) can also explain the pH dependence in Figure 5. At higher pH, $[H^+]$ can be omitted from the dominator and the reaction rate becomes independent on pH, i.e. limiting rate and the rate equation becomes;

$$\mathrm{Rate} = \frac{k_1[\mathrm{Zr{-}M^{n+}}]_0[\mathrm{H_2O_2}]_0}{[\mathrm{H_2O_2}]_0 + [\mathrm{Zr{-}M^{n+}}]_0} \quad (16)$$

With increasing $[H^+]$, *i.e.* decreasing pH, the rate becomes inversely proportional to $[H^+]$.

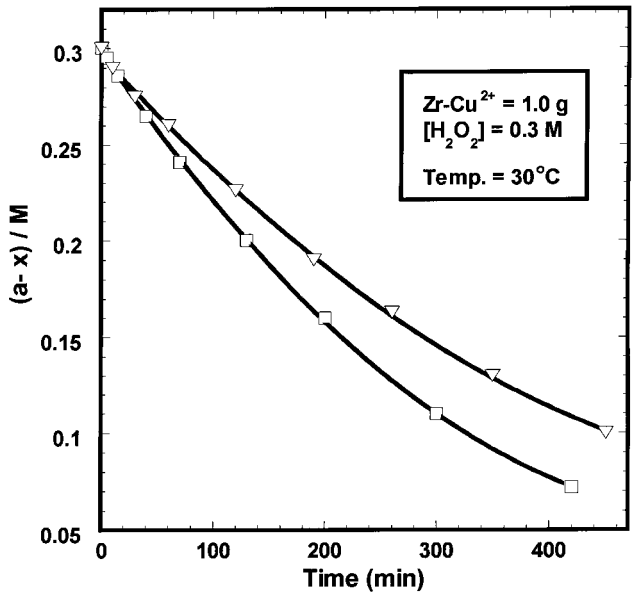

Fig. 4. Effect of *t*-BuOH scavenger on the decomposition of H_2O_2, (□); without scavenger and (△) 20% *t*-BuOH.

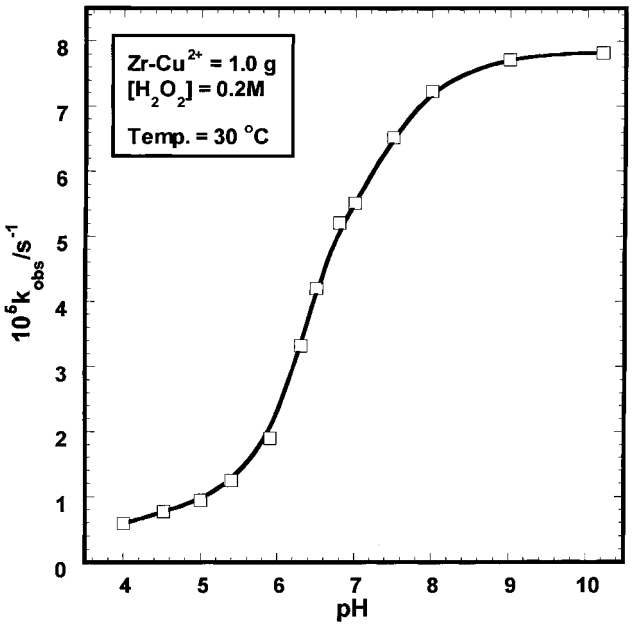

Fig. 5. Dependence of the observed rate constant on pH for the reaction of H_2O_2 with zirconia–Cu^{II}.

Conclusion

Zirconium(IV) oxide displays almost no catalytic activity towards hydrogen peroxide. However, when supported with transition metal ions, it becomes active, but the degree of activity is strongly dependent on the amount and the redox potential of the metal ion support, as well as on the pH of the medium. The order of reactivity depends on the initial concentration of hydrogen peroxide used. The degree of formation of the coloured intermediate at the early stages of the reaction is strongly dependent on the initial concentration of hydrogen peroxide and becomes marked at higher concentrations. The derived rate law is in agreement with the experimental results.

Acknowledgement

The Scientific Research Council of the United Arab Emirates University funded this research work.

References

1. J.C. Deutch, *Anal. Chem*., **255**, 1 (1998).
2. M.S. Reynolds, K.J. Babinski, M.C. Bouteneff, J.L. Brown, R.E. Campbell, M.A. Cowan, M.R. Durwin, T. Foss, P.O'Brien and H.R. Penn, *Inorg. Chim. Acta*, **263**, 225 (1997).
3. B.T. Hamstra, G.J. Colpas and V.L. Pecoraro, *Inorg. Chem*., **37**, 949 (1998).
4. M.H. Robbins and R.S. Drago, *J. Catal*., **170**, 295 (1997).
5. H. Tan and J.H. Espenson, *Inorg. Chem*., **37**, 467 (1998).
6. S.J. Yang and W. Nam, *Inorg. Chem*., **37**, 606 (1998).
7. A.E. Gekhman, I.P. Stolarov, N.I. Moiseeva, V.L. Rubaijlo, M.N. Vargaftik and I.I. Moiseev, *Inorg. Chem*., **275**, 453 (1998).
8. T.H. Zauche and J.H. Espenson, *Inorg. Chem*., **36**, 5257 (1997).
9. M. Uehara, M. Urade, A. Ueda, N. Sakagami and Y. Abe, *Bull. Chem. Soc*., **71**, 1081 (1998).
10. M.A. Kurbanov, N.A. Ibadov and Z.I. Iskenderova, *Kinet. and Catal*., **37**, 319 (1996).
11. M.M. Selim, M.K. El-Aiashi, H.S. Mazhar and S.M. Kamal, *Mater. Lett*., **28**, 417 (1996).
12. R. Neumann and M.L. Elad, *Applied Catalysts A*, **122**, 85 (1995).
13. V.A. Kirillov, N.A. Kuzin, V.N. Gavrilin and V.A. Kuz'min, *Kinet. and Catal*., **36**, 616 (1995).
14. J.A. Cox and K. Lewinski, *Talanta*, **40**, 1911 (1993).
15. B. Fubini, L. Mollo and E. Giamello, *Free Rad. Res*., **23**, 593 (1995).
16. A.H. Gemeay, M.A. Salem and I.A. Salem, *Coll. and Surf. A*, **117**, 245 (1996).
17. A.H. Gemeay, *Coll and Surf. A*, **116**, 277 (1996).
18. I.A. Salem, M.A. Salem and A.H. Gemeay, *J. Mol. Catal*., **84**, 67 (1993).
19. M.A. Salem, I.A. Salem and A.H. Gemeay, *Inter. J. Chem. Kinet*., **26**, 1055 (1994).
20. A.G. Govorov, A.B. Korzhenevskii, O.I. Koifman and T.G. Shikova, *Russ. J. Phys. Chem*., **69**, 1612 (1995).
21. P.C. Selvaraj and V. Mahadevan, *J. Mol. Catal. A*, **120**, 47 (1997).
22. R. Sreekala and K.K.M. Yusuff, *Ind. J. Chem*., **34A**, 994 (1995).
23. B. Beena, A. Shivanekar and U. Chudasama, *J. Mol. Catal. A*, **107**, 347 (1996).
24. M.Y. El-Sheikh, F.M. Ashmawy, I.A. Salem and A.B. Zaki, *Z. Phys. Chemie, Leipzig*, **269**, 126 (1988).
25. I.A. Salem, *J. Mol. Catal*., **80**, 1 (1993).
26. I.A. Salem, Inter. *J. Chem. Kinet*., **26**, 341 (1994).
27. I.A. Salem, Inter. *J. Chem. Kinet*., **27**, 499 (1995).
28. M.Y. El-Sheikh, F.M. Ashmawy, I.A. Salem and A.B. Zaki, *Transition Met. Chem*., **16**, 319 (1991).
29. I.A. Salem, M.Y. El-Sheikh, and A.B. Zaki, *Monatsh. Chem*., **126**, 393 (1995).
30. I.A. Salem, M.Y. El-Sheikh, and A.B. Zaki, *Inter. J. Chem. Kinet*., **26**, 955 (1994).
31. Y. Okamoto, K. Ohto and T. Imanko, *Kagaku Kogaku Ronbunshu*, **19**, 863 (1993).
32. Y. Okamoto and H. Gotoh, *Catalysis Today*, **36**, 71 (1997).
33. K.A. Bethke, D. Alt and M.C. Kung, *Catal. Lett*., **25**, 37 (1994).
34. R.A. Koeppel, A. Baiker and A. Wokaum, *Appl. Catal. A*, **84**, 77 (1994).
35. Y. Nitta, O. Suwata, Y. Ikeda, Y. Okamoto and T. Imanka, *Catal. Lett*., **26**, 345 (1994).
36. O. Suwata, Y. Ikeda, t. Fujimatsu, Y. Okamota and Y.Y. Nitta, *Kagaku Kogaku Ronbunshu*, **21**, 1009 (1995).
37. M. Anpo and S.C. Moon, *Res. Chem. Intermed*., **25**, 1 (1999).
38. *JCPDS-ICDD*, data base (1995).
39. I.A. Salem and S.A. Amer, *Transition Met. Chem*., **20**, 494 (1995).
40. J.D. Rush and W.H. Koppenol, *J. Inorg. Biochem*., **29**, 199 (1987).

TMCH 4569